Quan Wen, Yumei Yue, Shude Ji*, Zhengwei Li and Shuangsheng Gao

Effect of Welding Speeds on Mechanical Properties of Level Compensation Friction Stir Welded 6061-T6 Aluminum Alloy

DOI 10.1515/htmp-2014-0220
Received November 27, 2014; accepted March 12, 2015

Abstract: In order to eliminate the flash, arc corrugation and concave in weld zone, level compensation friction stir welding (LCFSW) was put forward and successfully applied to weld 6061-T6 aluminum alloy with varied welding speed at a constant tool rotational speed of 1,800 rpm in the present study. The glossy joint with equal thickness of base material can be attained, and the shoulder affected zone (SAZ) was obviously reduced. The results of transverse tensile test indicate that the tensile strength and elongation reach the maximum values of 248 MPa and 7.1% when the welding speed is 600 mm/min. The microhardness of weld nugget (WN) is lower than that of base material. The tensile fracture position locates at the heat affected zone (HAZ) of the advancing side (AS), where the microhardness is the minimum. The fracture surface morphology represents the typical ductile fracture.

Keywords: 6061-T6 aluminum alloy, level compensation friction stir welding, mechanical properties, fracture location

Introduction

Friction stir welding (FSW) is a new and promising solid-state joining technique that was invented at the Welding Institute (TWI) of the UK in 1991 [1, 2]. Since FSW has advantages of defect suppression, it is well suited for joining precipitation-strengthened aluminum alloys [3]. 6061-T6 aluminum alloy is one of moderate strength aluminum alloys and possesses excellent welding characteristics, which has been widely used in aerospace, automotive and railway industries [4, 5]. Liu et al. [6–8] showed that the tensile strength of the defect-free FSW joint of 6061-T6 aluminum alloy increases with increasing welding speed, and the maximum tensile strength is equivalent to 69% of the base material (BM). Heidarzadeh et al. [9] pointed out that the tensile strength and elongation of friction stir welded AA 6061-T4 joints increase with increasing rotational velocity and decrease with continuously increasing welding speed. In conventional FSW, it is well known that flashes, arc corrugation and concave are the typical defects, which are unfavorable for mechanical properties and beauty of joints [10–12]. Moreover, the existence of these defects easily causes local stress concentration [13]. However, the above-mentioned disadvantages can be easily eliminated by level compensation friction stir welding (LCFSW), which is put forward in this study. As a variation of conventional FSW, LCFSW is also a solid state joining technology. Before the LCFSW process, a small convex platform in weld zone is prefabricated. After welding, the convex platform would be removed using milling, and then the glossy joint with equal thickness of BM can be attained.

Extrusion technology can be widely used to manufacture the hollow structure of aluminum alloy. It is easy to get the hollow extrusion structure with small convex platform through the well-designed mold. In fact, the structure with small convex platform has been used for the field of transportation. For conventional FSW, in order to improve the beauty of joints, the milling cutter is always used to eliminate the flash after welding. With regard to LCFSW, the small convex platform should also be removed by milling cutter after welding, and the milling direction is contrary to welding direction. In view of the above-mentioned facts, it can be conclude that LCFSW is suitable for the batch production, which cannot increase the difficulty or complexity compared with conventional FSW. In this study, the difference of macrostructure between LCFSW and conventional FSW is investigated. Effects of welding speeds on hardness and mechanical properties of LCFSW joint of 6061-T6 aluminum alloy are discussed and analyzed in detail.

Experimental procedure

In the experiment, 4 mm thick 6061-T6 plates were used as BM. The plates have a small convex platform with 0.4 mm

***Corresponding author: Shude Ji,** Shenyang Aerospace University, No. 37, Daoyi South Avenue, Daoyi Development District, Shenyang 110136, China, E-mail: superjsd@163.com
Quan Wen, Yumei Yue, Zhengwei Li, Shuangsheng Gao, Shenyang Aerospace University, No. 37, Daoyi South Avenue, Daoyi Development District, Shenyang 110136, China

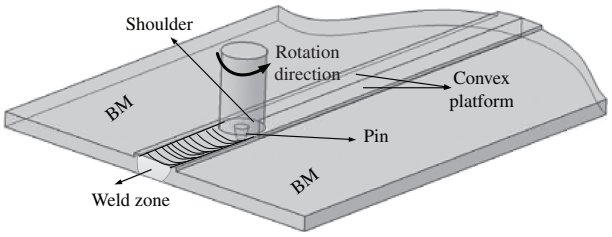

Figure 1: Schematic diagram of LCFSW.

thickness and 7 mm width in weld zone. The schematic diagram of LCFSW is illustrated in Figure 1. The small convex platform is regarded as compensation materials in weld zone. 6061-T6 aluminum alloy (1.1% Mg, 0.6% Si, 0.7% Fe, 0.25 Sn, 0.15% Cu, Mn, Ti and Al balanced) plates with dimensions of 300 mm × 50 mm were joined by FSW. Constant rotational speed of 1,800 rpm and welding speed of 200, 400, 600 and 800 mm/min were applied. Fabricated from H13 tool steel, the tool consists of a flat shoulder having a diameter of 10 mm and a pin with right hand screw. The pin is tapered from 4 mm at the pin bottom to 2 mm at the pin tip. The pin length used in LCFSW is 4.1 mm. For conventional FSW, the pin is 3.7 mm in length and the other geometric dimensions of tool are the same as LCFSW. During the LCFSW and conventional FSW process, the tool was operated at a tilt angle of 2.5° and the plunge depth was 0.2 mm. After welding, metallographic specimens were polished and then etched using modified Keller's reagent. Macrostructure observation of LCFSW joints was performed using optical microscopy (OM, Olympus GX71). The transverse tensile test specimens were cut by electrical discharge cutting machine. Transverse tensile test was carried out at room temperature using universal tensile machine with crosshead speed of 1 mm/min. In order to evaluate the mechanical properties of joints, average value of three tensile specimens was presented for discussion. After tensile experiment, the fracture morphologies of specimens were observed by a scanning electron microscopy (SEM, KYKY-2008B). The fracture locations were examined by OM. Microhardness profile along the transverse weld centerline was measured using Vickers hardness tester with a load of 100 g and a dwell time of 25 s.

Results and discussion

Macrostructure of the joints

The macrostructures of FSW and LCFSW joints are displayed in Figure 2. It can be seen that the material in

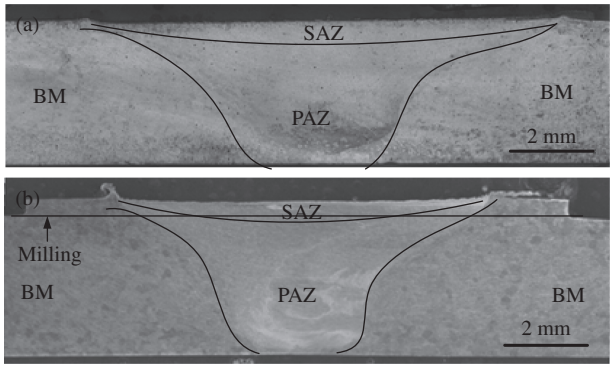

Figure 2: Macrostructure of joint: (a) conventional FSW and (b) LCFSW.

shoulder affected zone (SAZ) of conventional FSW is concave under the action of axial force (Figure 2(a)). The thickness of weld zone due to the formation of flash is lower than that of BM. Figure 2(b) shows the macrostructure of LCFSW joint before milling. In weld zone, the flash and concave are also formed. The thickness of weld zone is lower than the total thickness of small convex platform and BM, but higher than that of BM. After welding, the convex platform can be removed using milling, so the flash and arc corrugation are also eliminated, increasing the beauty of joint. Compared with BM, therefore, the equal thickness joint without flash and corrugation is attained. From Figure 2(a) and 2(b), it is also found that the SAZ was markedly reduced. The thermomechanically affected zone (TMAZ) and heat affected zone (HAZ) were slightly reduced.

Microhardness profile

The transverse microhardness profiles on the cross sections of the joints are shown in Figure 3. It is seen that the microhardness profiles under different welding speeds all exhibit W shape. The hardness profiles are corresponding to four distinct zones, i.e. weld nugget (WN), TMAZ, HAZ and BM. With respect to the LCFSW joints at different welding speed from 200 to 800 mm/min, although the WN experiences dynamic recrystallization (DRX) caused by plastic deformation and high temperature, the hardness of WN is lower than that of BM. The microhardness in the WN is higher than that of TMAZ or HAZ. The minimum hardness locates at the HAZ because of the softening phenomenon. During the welding process, the temperature on advancing side (AS) is higher than that on the retreating side (RS) because of the formation of flash and the difference of plastic

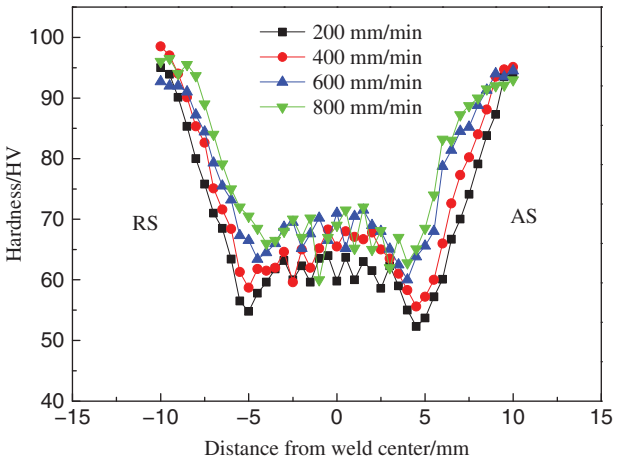

Figure 3: Microhardness profile of joints welded at different welding speeds.

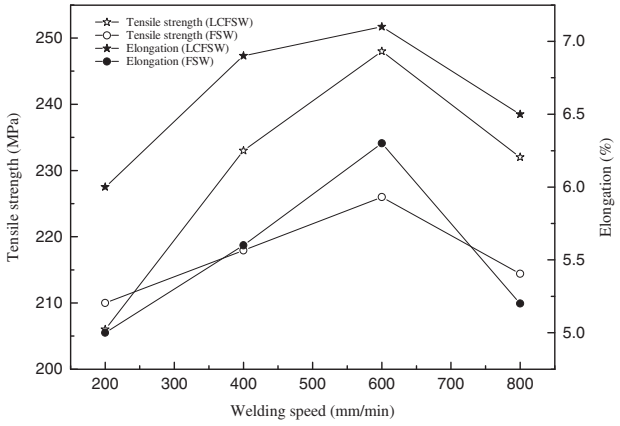

Figure 4: Tensile strength and elongation of LCFSW and FSW joints at different speeds.

deformation, which makes the microhardness of HAZ on AS lower than that on RS. Therefore, this hardness profiles in Figure 3 are asymmetry. With the increase of welding speed, the heat input in one unit decreases and the peak temperature of material in WN decreases, which results in the decrease of the width and softening degree of HAZ of welding joint. Moreover, under the constant rotational speed, the lower the peak temperature is, the finer the grains in WN are, which is beneficial for the increase of hardness. Therefore, the microhardness not only in HAZ but also in WN under the welding speed of 800 mm/min is higher than that under the lower welding speed varied from 200 to 600 mm/min.

Mechanical properties

The comparison of mechanical properties between LCFSW and conventional FSW is shown in Figure 4. It is observed that the mechanical properties of LCFSW and FSW show the same trends when the welding speed varies from 200 to 800 mm/min. During welding process, the frictional heat generated by shoulder and pin is related to the rotational speed and welding speed [14]. When the rotational speed of tool is constant, peak temperature in WN during the welding process is highest under the welding speed of 200 mm/min, resulting in the increase of the softening degree of and thus poor tensile strength and elongation of welding joints. With increasing the welding speed from 400 to 600 mm/min, peak temperature in WN decreases, which is beneficial for the decrease of softening degree and then results in the increase of mechanical properties of LCFSW joint. However, lower peak temperature means poor inadequate material flow, which may lead to cavity or lack of root penetration appear in WN and then deteriorate the quality of welding joint [15]. This may be the reason why the mechanical properties reduce when the welding speed further increases to 800 mm/min. The results of mechanical properties in this study are similar to that reported by Peel et al. [16]. In a word, under the constant rotational speed of 1800 rpm, the tensile strength of LCFSW joint increases firstly from 206 to 248 MPa and then decreases to 232 MPa. When the welding speed is 600 mm/min, the tensile strength and elongation of LCFSW joint both reach the maximum, whose values are, respectively, 248 MPa and 7.1%. The above-mentioned results show that there exists an optimum combination of the welding speed and the rotational velocity to produce a defect-free joint.

For FSW joint, WN can be divided into SAZ and pin affected zone (PAZ), as shown in Figure 2. During the welding process, the friction heat generated by shoulder is much more than that by pin. Therefore, temperature of material in SAZ is higher than that of pin, which results in the bigger DRX grains in SAZ. So, for defect-free joint, SAZ is weak area compared with PAZ. After the milling process for LCFSW, SAZ, HAZ and TMAZ are partly removed, which is beneficial for the mechanical properties. As mentioned above, material in WN is concave for the conventional FSW joint while the thickness of LCFSW joint is equal to that of BM. Therefore, compared with conventional FSW, the bearing area of LCFSW joint is bigger. Moreover, when the welding joint bears the tensile force, the existence of concave and arc corrugation easily causes the geometrical stress concentration, which goes against the quality of welding joint. The above-mentioned three reasons makes that the mechanical properties of LCFSW joint after removing the convex platform are higher than those of conventional FSW joint under the same welding parameters, as shown in Figure 4. In fact, some previous studies also investigated the tensile strength of conventional FSW joints of

6061 alloy [6–9, 17]. Heidarzadeh et al. [9] and Rajakumar et al. [18] attain the welding joint of conventional FSW with the maximum tensile strength of 159 and 224 MPa. The result reported by Liu et al. [6–8] is also lower than that in this study. Therefore, LCFSW is advantageous to improve the mechanical properties of welding joint.

Fracture of welding joint

The fracture locations of LCFSW joints are mainly discussed, as shown in Figure 5. It is seen from the figure that all the defect-free joints exhibit the obvious necking. It is well known that the tensile failure is likely to occur in the region with minimum hardness [18–20]. For LCFSW joint, the minimum microhardness locates at HAZ (Figure 3), so the fracture easily occurs in the HAZ adjacent to the TMAZ on AS, as shown in Figure 5. The material in SAZ experiences high temperature, which results in coarser grains and then possesses lower hardness. Therefore, the direction of fracture presents 45° from bottom surface to top surface and the final fracture position is located in SAZ. Because SAZ and HAZ of LCFSW joint are only partly removed by milling, the rest also owns lower or minimum microhardness compared with the other region of welding joint. Therefore, the fracture feature of conventional FSW joint in this study is similar to that of LCFSW joint, which is also reported by other researchers [7, 21]. Liu et al. [7] concluded that the fracture of the defect-free friction stir welded 6061-T6 joints occurs in the HAZ adjacent to the TMAZ. Wang et al. showed that the fracture of conventional FSW joints of 6061 aluminum alloy occurs in the HAZ and then the crack expands to the weld [21].

SEM micrographs of fracture surfaces of joints are shown in Figure 6. It is observed that all fracture surfaces of welding joints show dimples of varying size and depth, which represents the typical ductile fracture. The

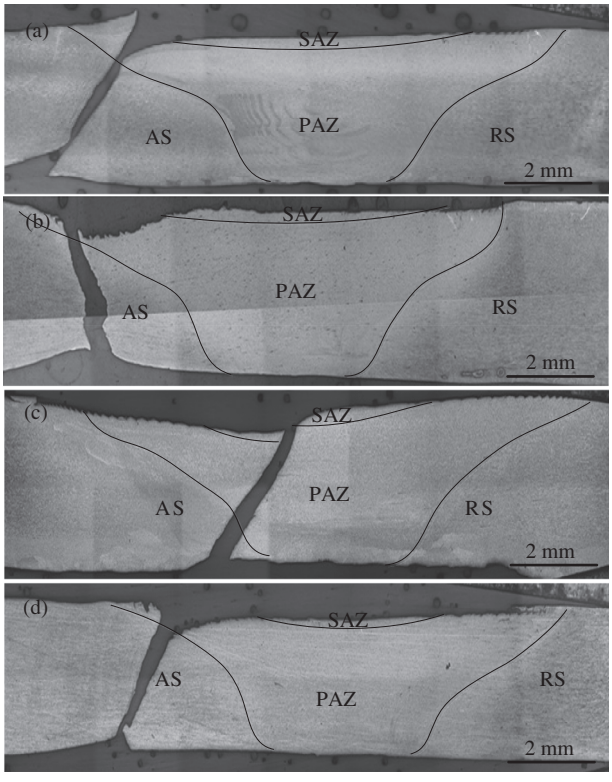

Figure 5: Fracture location of LCFSW welds at the rotational velocity of 1800 rpm with different welding speed: (a) 200 mm/min, (b) 400 mm/min, (c) 600 mm/min and (d) 800 mm/min.

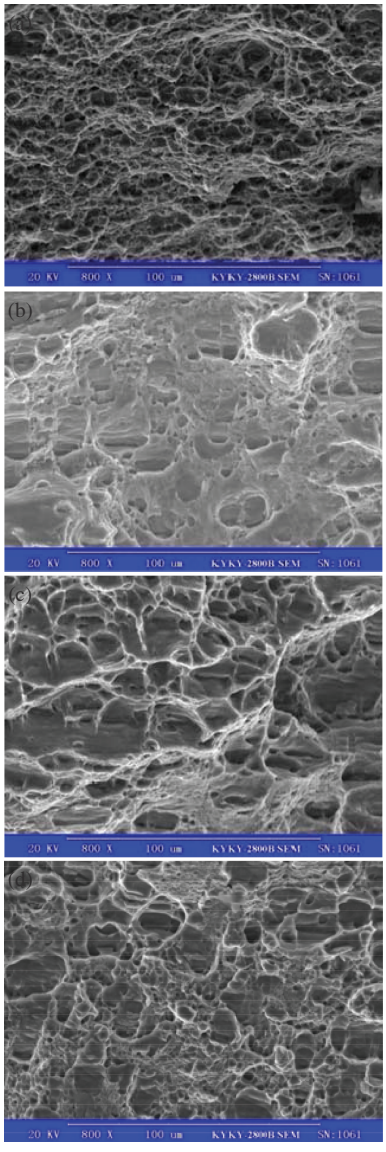

Figure 6: Fracture morphology of the joints welded at different welding speeds: (a) 200 mm/min, (b) 400 mm/min, (c) 600 mm/min and (d) 800 mm/min.

difference of fracture surfaces shows that the welding speed has significant effect on fracture morphology. Generally speaking, the higher the elongation of joint is, the better the ductility of joint is. Under the welding speed of 200 mm/min, the elongation of welding joint is lowest (Figure 4), so the fracture surface in Figure 6(a) is covered with shallower and smaller dimples, indicating the worst ductility. Under the welding speed of 400 and 800 mm/min, the elongations are both higher than that under the welding speed of 200 mm/min, which causes the increase of larger and deeper dimples (Figure 6(b) and 6(d)). From the viewpoint of dimple characteristics, it can be concluded that the ductility of joint under the welding speed of 600 mm/min is the best. In summary, the experimental results of fracture morphologies of LCFSW joints are in agreement with those of elongations.

Conclusions

6061-T6 aluminum alloy was successfully welded using LCFSW under different welding speeds. The following conclusions can be drawn from the present work.

1. By LCFSW technology, the glossy joint with equal thickness of the BM can be attained. The tensile fracture locations of LCFSW joint always show in HAZ of AS. The tensile strength and elongation of LCFSW joint are higher than those of conventional FSW under the same welding parameters.
2. When the welding speeds range from 200 to 800 mm/min, the tensile strength and elongation of LCFSW joints increase firstly and then decrease. Under the welding speed of 600 mm/min, the maximum tensile strength and elongation reach 248 MPa and 7.1%, respectively.
3. The microhardness profiles exhibit W shape and the minimum value locates in HAZ of AS. The microhardness of WN is lower than BM and increases with increasing the welding speed.
4. The fracture surface morphologies consisting of amounts of dimples indicate the ductile fracture. When the welding speed is 600 mm/min, the joint exhibits the best ductility.

Acknowledgments: This work was supported by the National Natural Science Foundation of China (No. 51204111), the Natural Science Foundation of Liaoning Province (Nos. 2013024004 and 2014024008), the Project of Science and Technology Department of Liaoning Province (No. 2013222007) and the Aeronautical Science Foundation of China (No. 2013ZE54021).

References

[1] P.L. Threadgill, A.J. Leonard, H.R. Shercliff and P.J. Withers, Int. Mater. Rev., 54 (2009) 49–93.
[2] R.S. Mishra and Z.Y. Ma, Mater. Sci. Eng. R., 50 (2005) 1–78.
[3] N. Afrin, D.L. Chen, X. Cao and M. Jahazi, Mater. Sci. Eng. A., 472 (2008) 179–186.
[4] J.Q. Zhang, Y.F. Shen, B. Li, H.S. Xu, X. Yao, B.B. Kuang and J.C. Gao, Mater. Des., 60 (2014) 94–101.
[5] C. Liu and X. Yi, Mater. Des., 46 (2013) 366–371.
[6] G. Liu, L.E. Murr, C.-S. Niou, J.C. Mcclure and F.R. Vega, Scripta Mater., 37 (1997) 355–361.
[7] H.J. Liu, J.C. Hou and H. Guo, Mater. Des., 50 (2012) 872–878.
[8] H.J. Liu, Y.C. Chen and J.C. Feng, Trans. Nonferrous Met. Soc. China, 15 (2005) 43–45 (in Chinese).
[9] A. Heidarzadeh, H. Khodaverdizadeh, A. Mahmoudi and E. Nazari, Mater. Des., 37 (2012) 166–173.
[10] J.W. Arbegast, Scripta Mater., 58 (2008) 372–376.
[11] H.B. Chen, K. Yan, T. Lin, S.B. Chen, C.Y. Jiang and Y. Zhao, Mater. Sci. Eng. A., 433 (2006) 64–69.
[12] H. Zhang, S.B. Lin, L. Wu, J.C. Feng and Sh.L. Ma, Mater. Des., 27 (2006) 805–809.
[13] G.Q. Wang and Y.H. Zhao, Friction Stir Welding of Aluminum Alloy, China Astronautic Publishing House, Beijing (2010) (in Chinese).
[14] J.F. Guo, H.C. Chen, C.N. Sun, G. Bi, Z. Sun and J. Wei, Mater. Des., 56 (2014) 185–192.
[15] R. Crawford, G.E. Cook, A.M. Strauss, D.A. Hartman and M.A. Stremler, Sci. Technol. Weld. Joining., 11 (2006) 657–665.
[16] M. Peel, A. Steuwer, M. Preuss and P.J. Withers, Acta Mater., 51 (2003) 4791–4801.
[17] S. Rajakumar, C. Muralidharan and V. Balasubramanian, Mater. Des., 32 (2011) 2878–2890.
[18] M.A. Sutton, A.P. Reynolds, J.H. Yan, B.C. Yang and N. Yuan, Eng. Fract. Mech., 73 (2006) 391–407.
[19] M.A. Sutton, A.P. Reynolds, B.C. Yang and R. Taylor, Mater. Sci. Eng., A., 354 (2003) 6–16.
[20] S.H.C. Park, Y.S. Sato and H. Kokawa, Scripta Mater. 49 (2003) 161–166.
[21] H.Y. Wang, W.J. Qi, D. Nong and F.Y. Zheng, Chin. J. Rare Met., 34 (2010) 638–642 (in Chinese).